Endocytosis and recycling of the complex between CD23 and HLA-DR in human B cells

SOPHIA N. KARAGIANNIS*, JOHN K. WARRACK†, KEVIN H. JENNINGS†, PAUL R. MURDOCK†,
GARY CHRISTIE†, KEVIN MOULDER†, BRIAN J. SUTTON* & HANNAH J. GOULD* *The Randall Centre for
Molecular Mechanisms of Cell Function, King's College London; †SmithKline Beecham Pharmaceuticals Ltd, New Frontiers
Science Park, Third Avenue, Harlow, Essex, UK*

SUMMARY

The presentation of extremely low doses of antigen to T cells is enhanced by immunoglobulin E (IgE)-dependent antigen focusing to CD23, the low-affinity receptor for IgE, expressed on activated B cells. CD23 contains a C-type lectin domain in its extracellular sequence and a targeting signal for coated pits, required for endocytosis, in its cytoplasmic sequence. CD23 is non-covalently associated with the major histocompatibility complex class II antigen, human leucocyte antigen HLA-DR, on the surface of human B cells, but the fate of this complex following endocytosis is unknown. To answer this question we have labelled these proteins on the surface of RPMI 8866 B cells and traced their route through the cytoplasm. Endocytosis mediated by anti-CD23 antibodies (BU38 and MHM6) led to the loss of CD23 from the cells. Endocytosis mediated by an antibody to HLA-DR (CR3/43) or an antigen–IgE complex (NP-BSA–anti-NP IgE), however, led to recycling of the HLA-DR–CD23 complex to the cell surface on a time scale (3–6 hr) consistent with the recycling of HLA-DR in antigen presentation. Along the latter pathway CD23 label was observed in cytoplasmic organelles that resembled the 'compartments for peptide loading' or 'class II vesicles' described by previous authors. Two features of the recycling process may contribute to the efficiency of antigen presentation. Peptide exchange may be facilitated by the proximity of HLA-DR and antigen in peptide loading compartments of the endosomal network. The return of CD23 with HLA-DR to the cell surface may then help to stabilize specific B-cell–T-cell interactions, contributing to T-cell activation.

INTRODUCTION

Human CD23 is a type II integral membrane protein of MW 45 000 that exists in two, separately regulated, isoforms (CD23a and CD23b), differing only in the 6/7 amino acids at the N terminus.[1,2] CD23a is expressed only in B cells following antigen activation, while CD23b is induced in a variety of cells by interleukin-4 (IL-4).[1] The activities of CD23 are dependent on this N-terminal sequence. CD23a in B cells mediates endocytosis, whereas CD23b in monocytes mediates phagocytosis.[3] The extracellular sequence of CD23 contains a C-type lectin domain, responsible for ligand binding, and an α-helical coiled-coil stalk, which leads to the formation of trimers in the cell membrane.[4–6]

CD23 has multiple ligands, including immunoglobulin E (IgE),[7,8] the integrins CD18/CD11b and CD18/CD11c[9] and the vitronectin receptor.[10] A well-characterized function of membrane-bound CD23 in B cells is the enhancement of IgE-dependent antigen presentation to T cells.[11–20] This requires the binding of antigen–IgE antibody complexes to CD23, internalization of the complexes, and transport to compartments of the endosomal network containing proteolytic enzymes and major histocompatibility complex (MHC) class II antigens. After digestion of the antigen, restricted peptides are loaded onto MHC class II antigens and returned to the cell surface for presentation to T cells. Antigen presentation also requires interaction between CD23 and CD21 at points of contact on the B- and T-cell surfaces.[21,22] Neither the fate of the internalized CD23 nor of IgE during antigen presentation are known. Another function of membrane-bound IgE, the feedback regulation of IgE synthesis,[23–26] may well be related to the endocytosis of antigen–IgE complexes and degradation of IgE within B cells.

An endogenous protease cleaves CD23 in the extracellular sequence to release a fragment of 37 000 MW containing the lectin domain and a large portion of the stalk.[27,28] Further proteolysis yields a stable 25 000 MW fragment, containing the

lectin domain and adjacent section of the stalk. This fragment binds to CD21 to promote the growth and differentiation of cells of the B-cell,[29,30] T-cell[31,32] and myeloid cell[33] lineages. This activity of CD23 is analogous to that of the C3 fragments of complement, which is also mediated by CD21 (also known as complement receptor 2).[34,35] When CD23 interacts with the integrins CD18/CD11b and CD18/CD11c (also known as CR3 and CR4, respectively) on monocytes, it stimulates the production of the pro-inflammatory mediators IL-1β, tumour necrosis factor-α (TNF-α) and IL-6 and nitrite oxidative products.[9] However, the present study focused on the behaviour of membrane-bound CD23a (hereafter termed simply CD23) in B cells.

Epstein–Barr virus (EBV)-transformed B-cell lines have served as a model system for CD23-facilitated antigen presentation.[12,13] In one such line, RPMI 8866, it has been shown that CD23 and the MHC class II antigen, human leucocyte antigen HLA-DR, are non-covalently associated in the cell membrane,[21,36] and contact sites in CD23 have been identified.[37] Facilitated antigen presentation begins with the capture of antigen–IgE complexes by CD23 on the cell surface and ends with the presentation of antigenic peptides bound to MHC class II antigens on the cell surface. We therefore predicted that co-localization of the transport proteins, CD23 (antigen donor) and HLA-DR (peptide recipient), in the endosomal network, and recycling of the ternary complex to the cell surface, might be mechanisms involved in the enhancement of antigen presentation by CD23.

To discover whether the complex between CD23 and HLA-DR remains intact during endocytosis, we examined RPMI 8866 cells exposed to antibodies against CD23 or HLA-DR or an antigen–IgE complex. We have used flow cytometry, coupled with acid-washing, to follow the internalization of the proteins, confocal microscopy to identify the intracellular locations, and immunoelectron microscopy to observe the fine structure of the intracellular compartments containing the proteins.

MATERIALS AND METHODS

Cell cultures

RPMI 8866 EBV-transformed lymphoblastoid cells were grown in suspension in RPMI-1640 medium with 10% heat-inactivated fetal bovine serum, 2 mM L-glutamine, 100 IU/ml penicillin, 100 μg/ml streptomycin at 37° under 5% CO_2/95% air in a humidified incubator. Tissue culture chemicals, media and phosphate-buffered saline (PBS) (Gibco-BRL) for live cell washes and antibody dilutions were fortified with 1·0 mM $CaCl_2$. Cell washings were carried out in medium by centrifugation at 200 *g* for 3·5 min at 4°. Paraformaldehyde or glutaraldehyde-fixed cells were centrifuged at 150 *g* for 5 min at room temperature.

Antibodies and other materials

Anti-CD23 antibody EBVCS1 was supplied by Dr Bill Sugden (University of Wisconsin, Madison, WI), EBVCS5 by Becton Dickinson, BU38 by Binding site Ltd. (Birmimgham, UK), I0B8 by Immunotech (Marseille, France) and B6 by Coulter Clone (Luton, UK). Murine monoclonal antibody (mAb) CR3/43 to HLA-DR and anti-mouse IgG (Fab′)₂-fluorescein isothiocyanate (FITC) were supplied by Dako Ltd.

(Cambridge, UK). The antibody IgG (Fab′)₂-Cy5 was from Chemicon International Inc. (Temecula, CA) and IgG Fab-R-phycoerythrin (PE) was from Southern Biotechnology Associates Inc. (Birmingham, AL). Colloidal gold conjugates were from British BioCell International (Cardiff, UK). The hapten 4-hydroxy-3-nitro-phenacetyl covalently conjugated to bovine serum albumin (NP-BSA) was a gift from Dr G. A. Mackay (King's College London).

Flow cytometry

Samples with 1×10^6 cells each were washed and incubated with a primary antibody (1 μg/ml) for 1 hr at 4°. Antibodies were previously tested to confirm they were used at optimal concentrations. Following two washes, all samples were incubated with 40 μg/ml anti-mouse IgG (Fab′)₂-FITC for 45 min at 4°. In experiments using double fluorophore labelling RPMI 8866 cells were incubated with the primary antibodies, followed by IgG Fab-R-PE, and a further incubation with a different antibody conjugated to FITC. Samples were washed three times and kept in medium for 0, 3 and 5 hr in a 37° incubator. Samples were washed once in PBS + 0·1% NaN_3, pH 7·2, to arrest cell growth and stop CD23 endocytosis. To remove surface fluorescence and measure the fraction of cells showing endocytosis, acid washing was performed in 150 mM NaCl and 20 mM HCl, pH 1·7, for 3 min at room temperature. A trypan blue exclusion test showed a loss of 5–10% of cells. After three washes, cells were fixed in 0·5 ml 2% paraformaldehyde/PBS/1% BSA/1 mM $CaCl_2$, pH 7·2, for 20 min at room temperature, washed in PBS/1% BSA/1 mM $CaCl_2$/0·02% NaN_3, pH 7·2, and fluorescence distribution was measured on a Becton-Dickinson flow cytometer.

Confocal microscopy

Samples, each with 5×10^5 cells, were washed once and incubated for 1 hr at 4° with 1 μg/ml mouse anti-human antibodies. After two washes, they were incubated in goat anti-mouse IgG (Fab′)₂-FITC (diluted 1 : 50 from stock) for 45 min at 4° and washed twice. In the IgE-antigen-induced endocytosis experiment, the cells were further incubated with 10 μg/ml NP-IgE[38] for 1 hr at 4°. They were washed three times and subjected to a further incubation with 10 ng/ml NP-BSA. In co-localization experiments, cells were incubated with anti-mouse IgG (Fab′)₂-Cy5 instead, followed by a further incubation with another antibody covalently conjugated to FITC. Cells in all the experiments described above were washed three times, suspended in medium and incubated in a 37° humidified incubator for 0, 2, 4, 6, or 8 hr. They were then washed twice in PBS and fixed in 2% formaldehyde/PBS, pH 7·2, for 15 min at room temperature. Following one wash in PBS, cells were suspended in 100 μl Citifluor/glycerol/PBS fluorescence preserver (Agar Scientific Limited, Stansted, UK). For observation, 10 μl of fixed cell suspension was combined with 5 μl DiBAC₄(5) (Molecular Probes, Eugene, OR) (1 mg/ml in methanol, diluted to 10 μg/ml in Citifluor) or with 5 μl propidium iodide (Sigma, Poole, Dorset, UK) (diluted to 1 μg/ml in PBS), on poly L-lysine-coated slides (BDH, Poole, UK). The slides were sealed with nail varnish and observed under a BioRad MRC600 confocal microscope.

Electron microscopy

Cells were divided into samples, each with $2 \cdot 4 \times 10^7$ cells, washed once and incubated for 2 hr in 3 ml medium with 1 µg/ml mouse anti-human antibody. After the first wash, cells were treated for 1 hr with anti-mouse IgG Fab bound to 5 nm gold (diluted 1 : 30 from stock). In double labelling experiments, cells were incubated with a second antibody, conjugated to biotin, followed with an incubation with anti-biotin antibody bound to 10 nm gold. All the above incubations were performed at 4° on a rocker. Cells were washed once and incubated for up to 10 hr at 37°.

Cells were then washed once and fixed in 2·5% glutaraldehyde/100 mM cacodylate buffer (Agar Scientific Limited), pH 7·2, for 2 hr at 4°. After one wash in 100 mM cacodylate buffer, they were treated in 1% osmium tetroxide/100 mM cacodylate buffer (Agar Scientific Limited) for 45 min at room temperature. Samples were washed twice, suspended in 200 µl of 4% BSA/50 mM Tris/150 mM NaCl, pH 7·4, and 20 µl of 25% glutaraldehyde to cross-link BSA and produce a gel-like pellet. Cells were mixed and centrifuged for 5 min at 500 $\mathbf{g}$. The cell pellets were placed in 30% ethanol and cut into 1 mm^3 cubes. The cubes were dehydrated in 50, 70, 90 and 95% ethanol by gentle rotation for 15 min each rinse and for three 10-min intervals in 100% ethanol.[39] They were suspended in 50% LR White resin (London Resin Company – distributed by Agar Scientific Limited)-50% ethanol, rotated for 1 hr, then in LR White (London Resin Company) and rotated overnight at room temperature. Resin-embedded samples were placed in gelatin capsules and kept at 52° for 24 hr. Ultrathin sections of 50–70 nm thickness were cut and mounted on nickel grids, stained in uranyl acetate for 1·5 min and washed with distilled water, followed by an incubation in lead citrate for 2 min. Sections were rinsed in distilled water, dried and observed under a Hitachi H7100 electron microscope.

Electrophoretic analysis of recycled CD23

Cells were iodinated by the lactoperoxidase method as previously described,[40] followed by two washes in PBS and one in medium and resuspended in medium at 1×10^6 cells/ml. They were incubated at 37° with 100 µl CR3/43 per ml medium or 100 µl of medium alone (control) in a humidified incubator for 18 hr. The cells were then subjected to protease treatment or acid washing or untreated (control), followed by lysis and immunoprecipitation. Aliquots of iodinated cells were washed three times in PBS, resuspended in 500 µl chymotrypsin/PBS (5 mg/ml stock) (Calbiochem, Nottingham, UK) and incubated on ice for 10 min. Fetal calf serum was then added to limit the protease digestion and cells were centrifuged at 2000 $\mathbf{g}$ for 1 min in 1 ml 50% FCS/PBS and then in 1 ml PBS. The cell pellet was collected and subjected to lysis and immunoprecipitation. Aliquots of iodinated cells were washed three times in PBS and resuspended in 500 µl acid wash buffer (140 mM NaCl/10 mM sodium citrate/50 mg/ml BSA, pH 2·8). The cells were incubated at 25° for 10 min and centrifuged at 2000 $\mathbf{g}$ for 1 min, followed by removal of the supernatant. The acid incubation and centrifugation steps were then repeated and the cell pellet was collected and subjected to lysis and immunoprecipitation.

The iodinated cells, as controls, or cells subjected to protease treatment or to acid washing, were lysed by addition of 750 µl lysis buffer [50 mM Tris/150 mM NaCl/0·5% nonidet

P-40 (NP-40)/5 mM ethylenediaminetetraacetic acid, pH 8] to the cell pellet, followed by incubation on ice for 30 min The lysed cells were centrifuged at 2500 $\mathbf{g}$ for 15 min and the supernatant was added to antibody BU38, which had been previously incubated at 25° for 1 hr with protein A agarose beads (GibcoBRL, Life Technologies, Paisley, UK). The lysed cell supernatant and anti-CD23 agarose beads were incubated at 25° for 1 hr, and the beads were centrifuged three times in lysis buffer. The samples were analysed by polyacrylamide gel electrophoresis and autoradiography. The immunoprecipitate beads were added to 120 µl electrophoresis sample buffer (125 mM Tris/10% glycerol/2·4% sodium dodecyl sulpjate /5% 2-mercaptoethanol) and samples were heated at 80° for 15 min. They were centrifuged at 2500 $\mathbf{g}$ for 5 min and 100 µl of the supernatant was loaded onto a 13·5% polyacrylamide slab gel and run at 15 mA for 15 hr using a Bio-Rad Protean II system (Bio-Rad Laboratories Ltd, Hemel Hempstead, UK). The dried gel was placed against hyperfilm (Amersham Life Science Limited, Amersham, Bucks., UK) in an intensifier cassette for 3 days at −70° before developing.

RESULTS

Endocytosis of CD23 by anti-CD23 antibodies

Six anti-CD23 mAb were screened at saturating concentrations for their ability to enhance endocytosis of CD23 (Fig. 1). Our preliminary studies indicate that antibody-induced endocytosis of CD23 is relatively slow, taking at least 2 hr for extensive capping to occur. A flow cytometric assessment of the percentage of cells with significant internal fluorescence shows that BU38 is the most efficient, with 48% and 53% of cells exhibiting internal fluorescence after 3 and 5 hr at 37°, respectively. Antibody MHM6 enhanced endocytosis by 41 and 27% after 3 and 5 hr, respectively, while other antibodies, IOB8, B6, EBVCS1 and EBVCS5 were much less efficient. Incubations with all antibodies for 3 and 5 hr in ice showed that 95% of cells were negative for internal fluorescence (results not shown).

The stimulatory antibodies, BU38 and MHM6, bind to the lectin domain of CD23 and block IgE binding.[41] Two other antibodies, IOB8 and B6, which bind to the lectin domain and
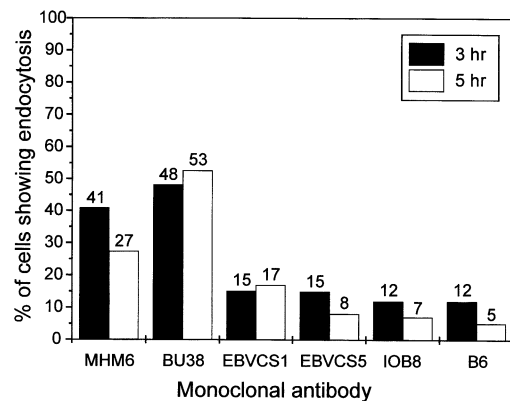

Figure 1. Flow cytometric comparison of the induction of endocytosis in RPMI 8866 cells by various anti-CD23 antibodies. The percentage of internalized CD23 with the various antibodies are indicated after 3 and 5 hr. Each measurement was the average of at least two experiments. Errors were typically ± 5%.

block IgE binding,[42] one antibody, EBVCS5, which binds to the lectin domain and does not block IgE binding,[42] and one, EBVCS1, which binds to the stalk of CD23,[42,43] all failed to stimulate the endocytosis of CD23. Thus we have shown that a subpopulation of antibodies against the lectin domain induce the endocytosis of CD23.

Induction of capping and endocytosis of CD23 by BU38 and MHM6

FITC-labelled BU38 induced capping of CD23 on the B-cell surface, followed by internalization and intracellular localization of CD23, as observed by confocal microscopy (Fig. 2). Cells kept in ice for 8 hr exhibit surface fluorescence and some antibody-induced cross-linking of CD23, manifested by the onset of capping on the cell periphery (Fig. 2a). After 2 hr at 37°, more extensive capping is observed and fluorescent indentations from the capped areas extend towards the cytoplasm, indicating the initiation of antibody-induced endocytosis (Fig. 2b). Extensive internal fluorescence, mostly detached from surface areas, is seen after 4 hr at 37° (Fig. 2c). Green fluorescence is localized within the cytoplasm and is clearly separate from the nucleus. After 4–6 hr at 37°, fluorescence appears to be contained in cytoplasmic regions adjacent to the nucleus (Fig. 2c,d). Surface fluorescence is decreased and capping is rarely observed. After 8 hr at 37°, the intensity of the fluorescent cytoplasmic regions is notably decreased and in most cells hardly visible (Fig. 2e). Surface fluorescence is also substantially diminished and capping is rare. These results suggest the possibility that CD23 may be degraded in the cells.

Visualization of CD23 in an endosomal compartment

Electron micrographs confirm the endosomal accumulation of internalized anti-CD23 antibody (Fig. 3). Endocytosed 5 nm gold-bound MHM6 antibody, marking the CD23 lectin domain, is seen originally in plasmalemmal pits (cells kept at 4°, Fig. 3a, small arrows) and later in cytoplasmic bodies that are rich in membranes and small structures (cells incubated at 37° for 10 hr, Fig. 3b, small arrows). These vesicles are often localized in groups in close proximity to each other and adjacent to the nucleus. Gold is seen in aggregates within this vesicular network. Similar results were obtained with BU38 (Fig. 3c–e). Cytoplasmic organelles of comparable appearance have been previously identified as components of the lysosomal network.[44] Endocytosed gold aggregation in lysosomes, and to a lesser extent in endosomes, has been reported in previous studies of gold-conjugated cell surface proteins.[44] Aggregation occurs as the protein coat that surrounds the gold particles is digested in late endosomes and lysosomes, resulting in flocculation of the gold colloid particles at low pH. These results extend the evidence from flow cytometry and confocal microscopy, indicating that BU38 and MHM6 may target CD23 into a degradative pathway in the cells.

Co-localization of the lectin domain and the stalk in endosomal vesicles

In a double immuno-gold labelling experiment, 5 nm gold Fab-EBVCS1 was bound to the stalk region of CD23 and the lectin domain was labelled with BU38-biotin, followed by anti-biotin
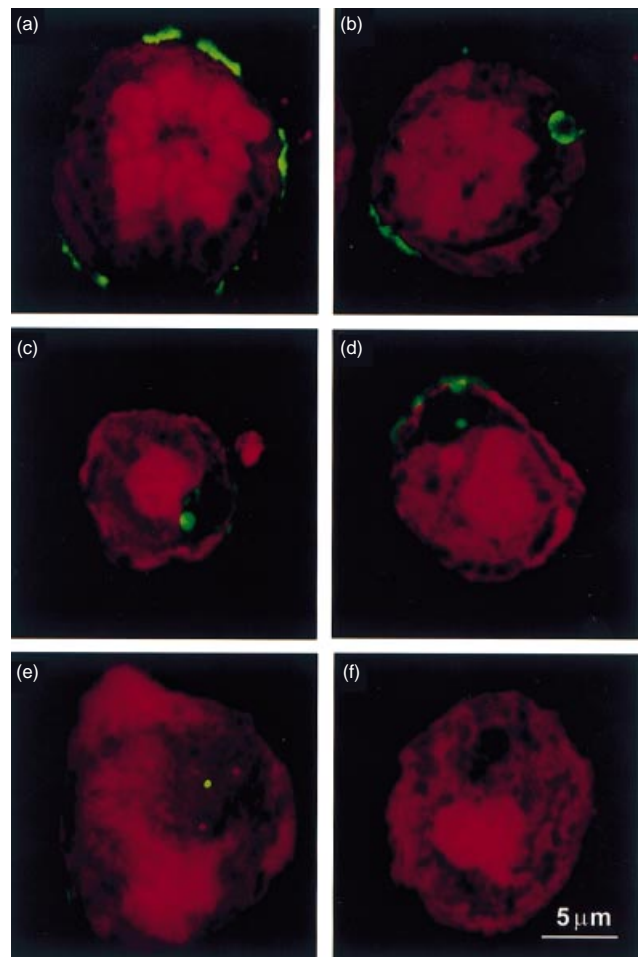

Figure 2. Confocal optical sections revealing the location of CD23 in RPMI 8866 cells, incubated with the anti-CD23 antibody, BU38. Samples were incubated with mouse anti-human antibody BU38, followed by goat anti-mouse IgG (Fab′)$_2$-FITC (green). Cells were labelled with propidium iodide (red), a nuclear stain, here used for the purposes of highlighting the cell structure. The thickness of optical sections was ∼1 μm. A sample was kept in ice for 8 hr (a), while others were incubated at 37° for (b) 2 hr, (c) 4 hr, (d) 6 hr and (e) 8 hr, to reveal capping (a, b) and internalization (b–e) of CD23. A control (f) shows the lack of non-specific surface labelling in cells incubated with the goat anti-mouse IgG (Fab′)$_2$-FITC but without BU38, and kept on ice for 8 hr. Furthermore, negative controls using mouse anti-human antibodies to proteins not expressed by RPMI 8866 cells such as LFA-1 mouse anti-human antibody to CD21 (Serotec, UK) followed by anti-mouse IgG (Fab′)$_2$-FITC showed lack of non-specific binding to cells (not shown).

bound to 10 nm gold (Fig. 3c–e). Cells incubated for 3·5 hr show gold in cell membrane invaginations fusing with early endosomes (Fig. 3c, long arrow). Gold particles of 5 nm (small arrowhead) and 10 nm (large arrowheads) are visible on the cell membrane and in early plasmalemmal structures (Fig. 3d). After 10 hr at 37° (Fig. 3e) gold labels for the lectin and stalk regions of CD23 are accumulated within tubular substructures in endosomal compartments, multivesicular structures and lysosomes (Fig. 3e, small arrows). All other cytoplasmic structures, such as Golgi cisternae and mitochondria, are free of gold labelling. A large fraction of the gold in these vesicles
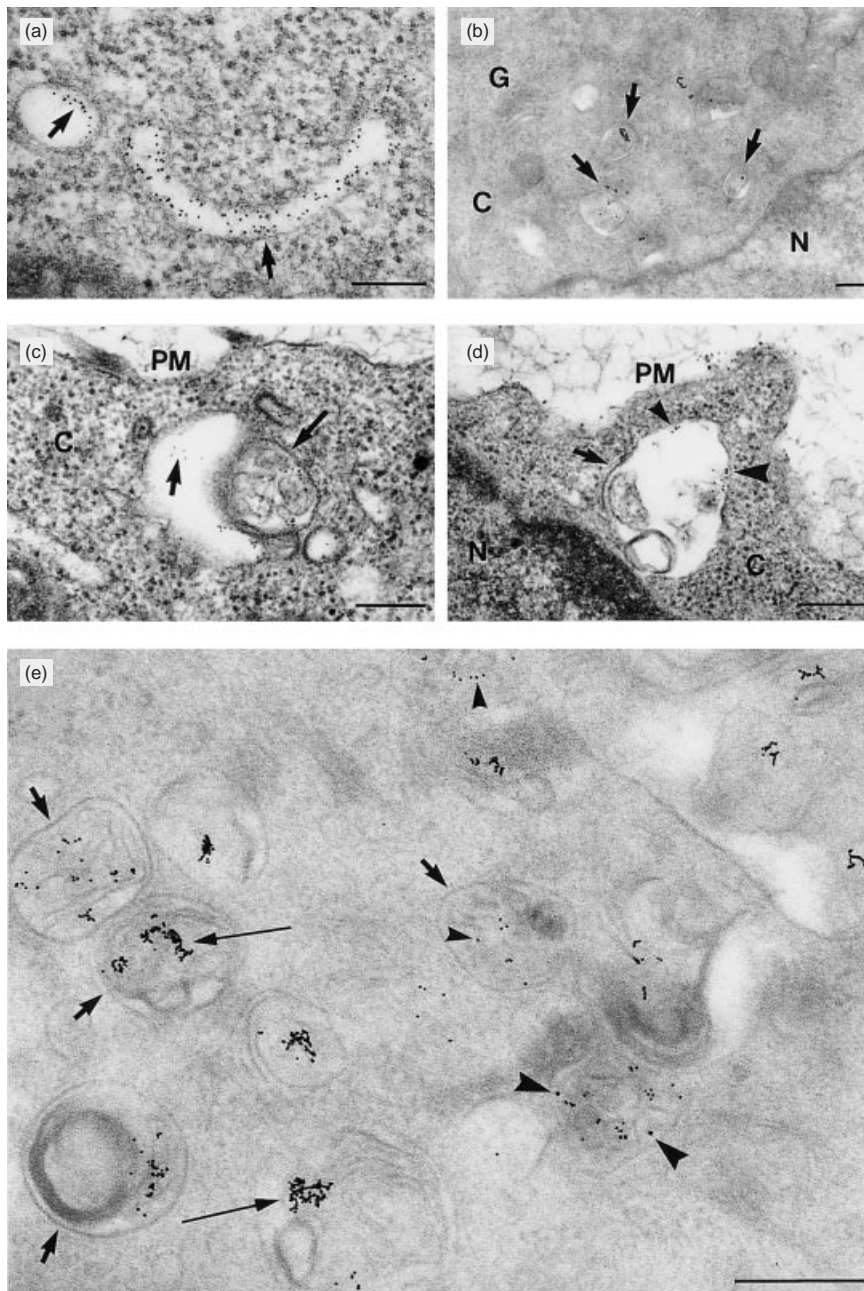
Figure 3. Electron microscopic visualization of CD23 domains, on antibody-induced endocytosis in RPMI 8866 cells. RPMI 8866 cells were incubated with the anti-CD23 lectin domain MHM6, followed by anti-mouse IgG, conjugated to 5 nm gold (a,b). Samples were incubated at 4° (a) and at 37° for 10 hr (b). Gold is accumulated within plasmalemmal pits (a, small arrows) and multivesicular cytoplasmic bodies, located in the region of the nucleus after 10 hr (b, small arrows). In another experiment, cells were incubated with the anti-CD23 stalk antibody, EBVCS1, followed by anti-mouse IgG Fab, conjugated to 5 nm gold to label the stalk, and with biotinylated BU38 followed by anti-biotin mAb, conjugated with 10 nm gold, to label the lectin domain (c–e). Cells were incubated at 37° for 3·5 hr (c,d) and 10 hr (e). Cell membrane indentations are seen after 3·5 hr (c,d small arrows), in close proximity to early endosomes (c, large arrow). Early vesicles contain 5 (d small arrowhead) and 10 (d, large arrowhead) nm gold. Following 10 hr at 37° (e) gold is accumulated mostly in aggregates (e, long thin arrows), within multivescicular cytoplasmic bodies (e, small arrows). The 5 nm gold particles representing the stalk domain (e, small arrowheads) are more prevalent than the 10 nm gold particles representing the lectin (e, large arrowheads). Cell sections in (a), (c) and (d) were labelled with uranyl acetate and lead citrate. Cell sections in (b) and (e) were unstained to confirm the presence of gold in the vesicles. C, cytoplasm; N, nucleus; G, golgi apparatus; PM, plasma membrane: scale bars = 250 nm.

was aggregated (Fig. 3e, long thin arrows), revealing that both the CD23 lectin and stalk domains may reach an acidic compartment. These results suggest that CD23 remains intact until it reaches endosomal compartments, where it undergoes proteolysis.

Simultaneous internalization of CD23 and HLA-DR

A FITC-labelled antibody against HLA-DR (CR3/43) was used to internalize HLA-DR and the fate of CD23 was followed by surface labelling with the antibody IOB8 and a secondary antibody Fab conjugated to R-PE. IOB8 was chosen because it was shown previously to cause minimal internalization of CD23 on its own. The two proteins were followed by two-colour flow cytometric measurements (Fig. 4). Dot plots demonstrate the intracellular location of both antigens and a slight excess of free HLA-DR. In a sample kept in ice, the cell population displays labelling for both antigens, as 86% fall within the upper right quadrant, representing dual fluorescence distribution (Fig. 4a). After acid stripping of extracellular protein, the threshold gates were set so that 86% of cells fall within the lower left quadrant and are thus considered negative for both FITC and R-PE (Fig. 4b). After 3 and 6 hr at 37°, 82–83% of cells register positive for total cell-associated FITC and R-PE (Fig. 4c at 3 hr). An acid washed sample (Fig. 4d)

indicates that cells display internal fluorescence for both antigens. Analysis reveals that 39% of cells are positive for both internal CD23 and HLA-DR and 15% for internal HLA-DR only. A negligible number of cells (0·08%) register positive for internal CD23 only. After 6 hr at 37° (Fig. 4f), 44% of cells register positive for internalized CD23 and HLA-DR together, whereas 9% are positive for internal HLA-DR and a negligible percentage of cells are positive for internal CD23 alone. These results demonstrate that the majority of cells internalize CD23 at the same time as HLA-DR.

Intracellular co-localization of CD23 and HLA-DR

Three-colour confocal microscopy was used to study the co-localization of HLA-DR and CD23 on the surface and in the cytoplasm of RPMI 8866 cells (Fig. 5). HLA-DR was followed by CR3/43, tagged with FITC (green), and CD23 by EBVCS1, tagged with Cy-5 (white). In a sample kept at 4° (0 hr), CD23 and HLA-DR are located together in distinct patches on the cell periphery. After 2 hr at 37°, both proteins are accumulated in capped areas on the cell periphery and their endocytosis is seen in cytoplasmic indentations. Following 4 hr at 37°, both fluorophores are co-localized in the cytoplasm close to the nucleus. Capping on the cell surface is considerably less pronounced, as endocytosis of both proteins progresses. Whereas HLA-DR without CD23 is also occasionally seen, CD23 is not seen on its own, consistent with the results of two-colour flow cytometry after acid stripping (Fig. 4d,f). This is also consistent with the previous observation that EBVCS1 fails to induce endocytosis of CD23. After 6 hr at 37°, intra-cellular location of CD23 and HLA-DR is clearly less evident (Fig. 5). Surface fluorescence is observed in patches showing the labels for both proteins. In some cells, a small trace of the Cy5 is left within the cell but no cytoplasmic accumulation of either fluorophore is observed. Reappearance of HLA-DR together with CD23 at the cell surface, after internalization by CR3/43, implies possible recycling of the complex in B cells.

Thus cross-linking of CD23 by the anti-CD23 lectin domain antibody (BU38) led to degradation of CD23 in the endosomal network (Fig. 2). Cross-linking of HLA-DR by CR3/43 led to internalization of the associated CD23 and our data suggest recycling of the complex to the cell surface (Fig. 5).

Targeting of HLA-DR–CD23 complexes to distinctive cytoplasmic vesicles

CD23 on RPMI 8866 cells was labelled with antibody IOB8 and anti-murine IgG Fab bound to 5 nm gold and HLA-DR was cross-linked with CR3/43. In samples kept in ice, electron micrographs (Fig. 6a) reveal strong cell surface capping and membrane invaginations (small arrows), indicating the onset of endocytosis. Following incubation for 3·5 hr at 37° (Fig. 6b,c), 5 nm gold is found, both in the area close to the cell membrane as well as further into the cytoplasm in gold-containing cyto-plasmic bodies, from plasmalemmal pits (Fig. 6b,c, small arrows) to more structured vesicles resembling primary endo-somes (Fig. 6b, large arrow). The endocytosed gold is sharp in appearance, indicating that it may have not been processed in an acidic and/or proteolytic environment. In some plasma-lemmal pits bearing gold associated with their inner mem-branes, the membrane appears to detach itself from the
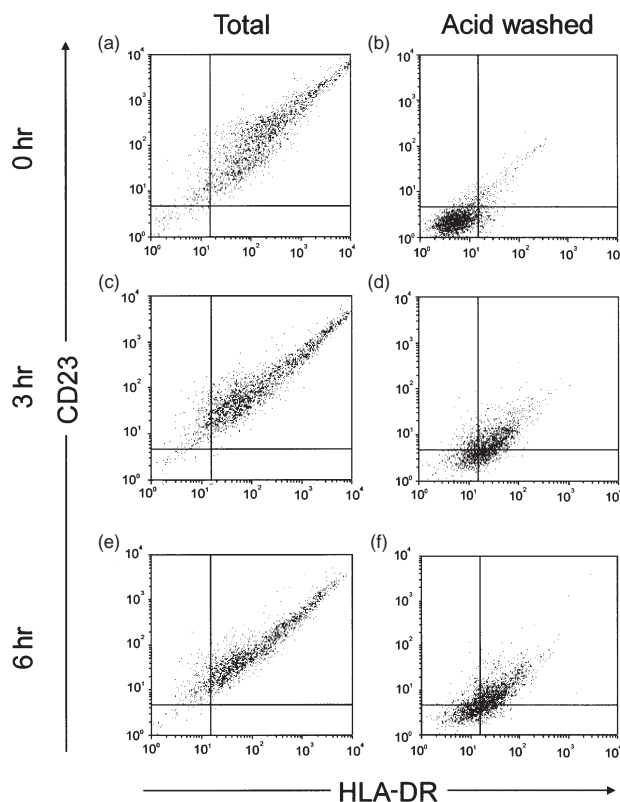

Figure 4. Co-internalization of HLA-DR and CD23, observed by flow cytometry of acid-washed RPMI 8866 cells. Cells were incubated with CD23 antibody, IOB8, and anti-mouse IgG Fab-R-PE, followed by anti-HLA-DR antibody CR3/43-FITC. Dot plots are divided into four quadrants, defined by the acid-washed controls (b). Sample incubated on ice (a,b) and at 37° for 3 hr (c,d) or 6 hr (e,f).
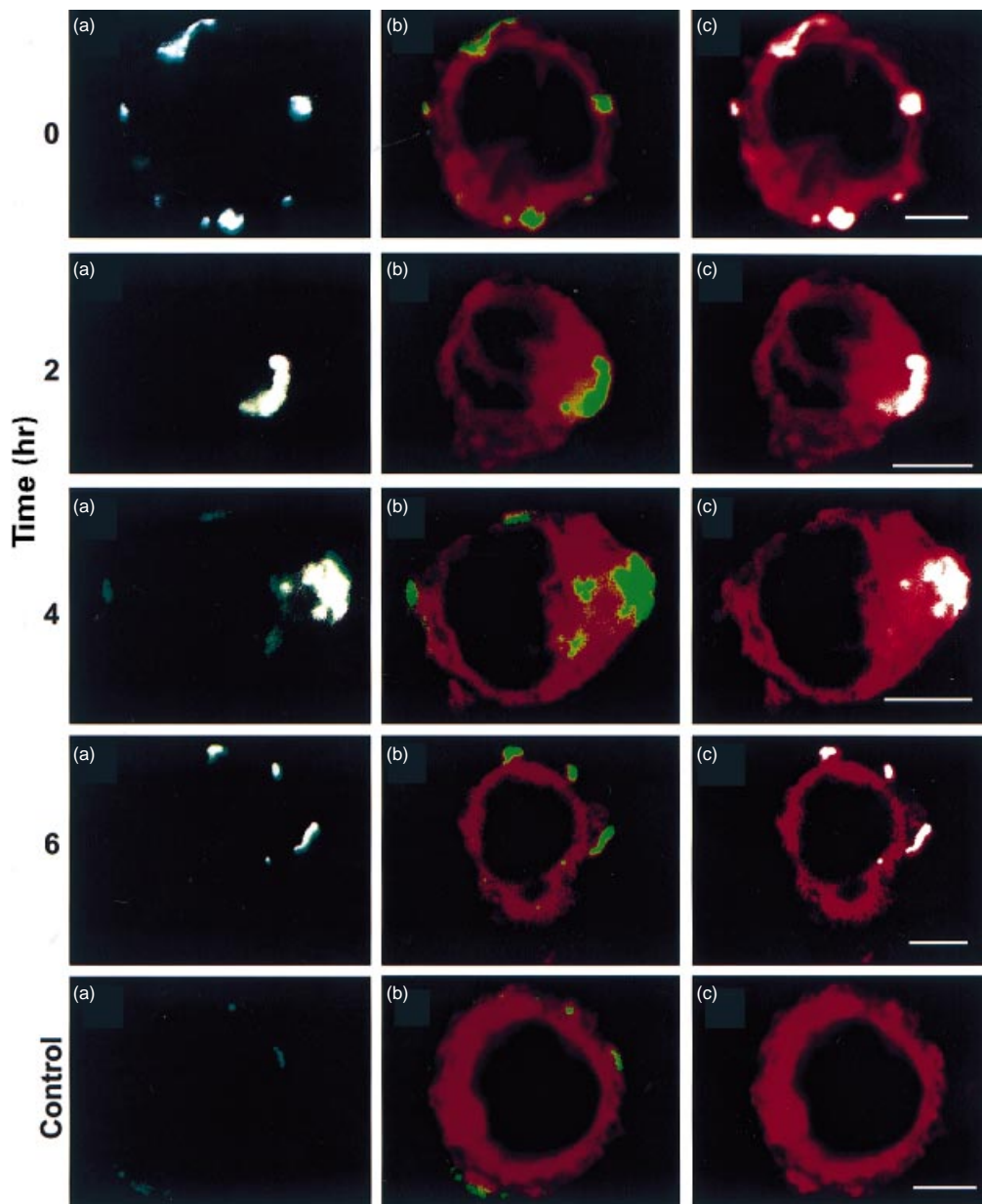
Figure 5. Three-colour confocal optical section displaying CD23 and HLA-DR in RPMI 8866 cells. Cells were incubated with the mouse anti-human CD23 antibody, EBVCS1, and anti-mouse IgG (Fab′)$_2$-Cy5, followed by anti-HLA-DR CR3/43-FITC. DiBAC$_4$(5) was used to highlight surface and cytoplasmic membranes but does not label the cell nuclei. Optical section thickness: ∼1 μm. Cells were kept on ice or incubated at 37° for 2, 4, or 6 hr. A negative control (c, marking the bottom row), kept on ice, contained the secondary antibody anti-mouse IgG (Fab′)$_2$-Cy5. Vertical panels represent (a) HLA-DR (green) and CD23 (white), (b) HLA-DR (green) and cytoplasmic membranes (red) and (c) CD23 (white) and surface and cytoplamic membranes (red).

remaining structure, and emerge as a new vesicle (Fig. 6c, large arrow). Such budding vesicles may be responsible for delivering CD23 to the endosomal network.

After 10 hr at 37°, gold particles are seen in vesicles in the cytoplasmic area close to the nucleus (Fig. 6d–f). Gold particles are detached from the membrane and form aggregates, indicating that CD23 has encountered acidic and proteolytic conditions (Fig. 6d, long thin arrows). Some gold-containing cytoplasmic bodies (Fig. 6d–f) appear similar to those observed in previous experiments (Fig. 3), with multilammenal and multivesicular structures, indicating that CR3/43 enhances

endocytosis of CD23 and delivery to endosomal and lysosomal compartments. Aggregated gold particles found in multi-lamenal and multivesicular bodies, are identified as components of the endosomal network (Fig. 6e,f, small arrowheads). However, aggregated gold is also observed contained in a novel vesicle (Fig. 6e,f, large arrowheads) with a structure distinct from others observed in antibody-induced endocytosis experiments. It features a multilayered membrane, resembling a coiled rope, and often a plain core inner structure.

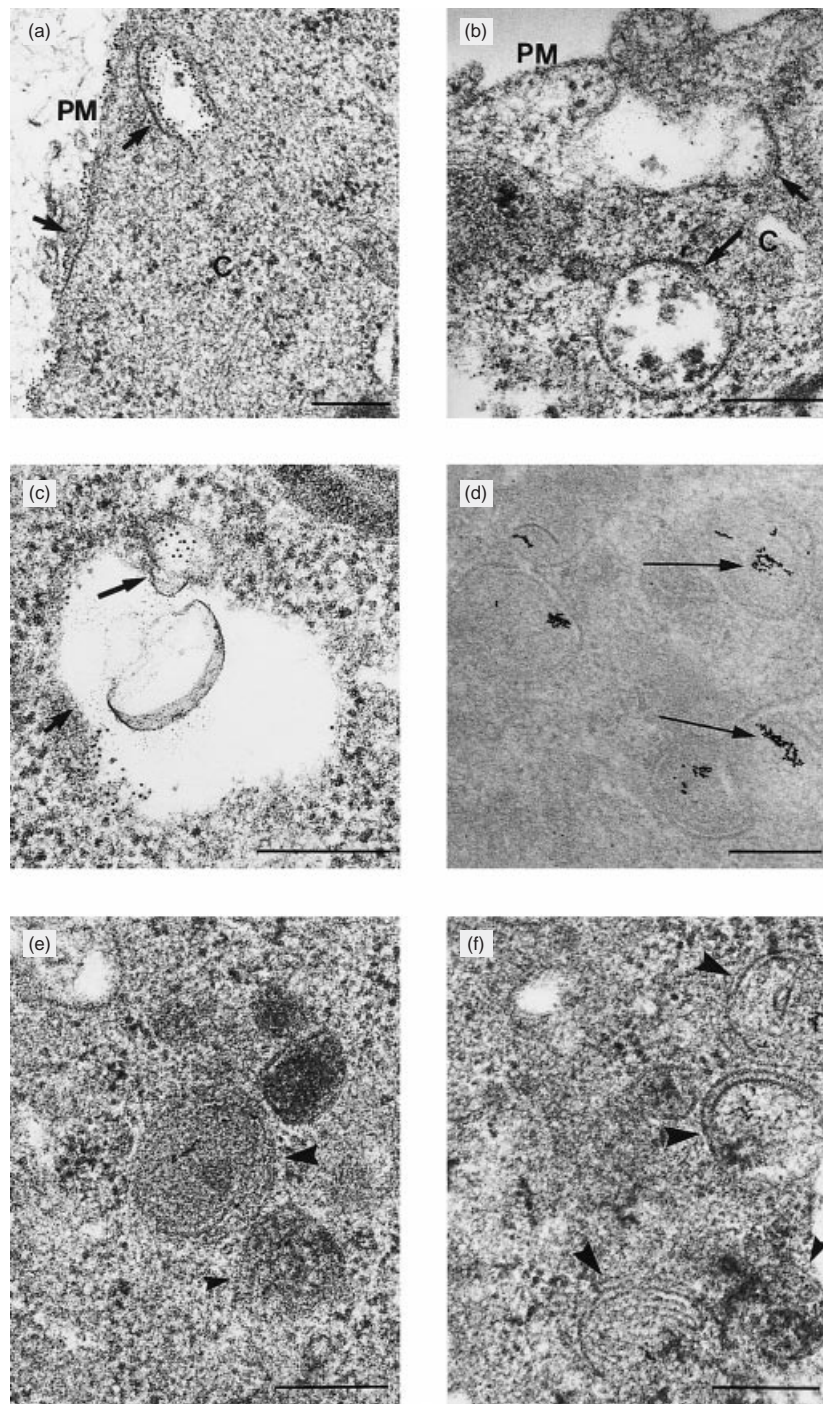Our interpetation of these micrographs is that endocytosis induced by antibody CR3/43 may divert the HLA-DR–CD23

Figure 6. Electron microscopic visualization of anti-HLA-DR endocytosis of CD23. RPMI 8866 cells were labelled with IOB8 and goat anti-mouse IgG Fab, conjugated to 5 nm gold, followed by the anti-HLA-DR antibody CR3/43. Sections in (a), (b), (c), (e) and (f) were stained with uranyl acetate and lead citrate to enhance vesicle structure. The unstained section in (d) was used to confirm the presence of aggregated gold in the vesicles. (a) Sample kept on ice: small arrows point to surface molecules and to plasmalemmal pits. Samples incubated at 37° for 3·5 hr (b,c) or 10 hr (d–f). (b) Gold in plasmalemmal pits (small arrow) and an early endosome (large arrow); (c) gold-filled vesicle (large arrow) budding from plasmalemmal pit (small arrow); (d) aggregated gold particles (long thin arrows) in multivesicular cytoplasmic bodies, located in groups within the cell cytoplasm; (e,f) groups of multivesicular bodies containing aggregated gold (arrowheads). Some vesicles have a coiled rope motif (large arrowheads) and others do not (small arrowheads). C, cytoplasm; PM, plasma membrane: scale bars = 250 nm.

complex into a different pathway from that followed by complexes internalized by BU38 or MHM6 (the antibodies that compete with IgE). The gold inside these bodies is aggregated and lacks the sharpness of membrane-bound gold, suggesting an acidic environment similar to that found in late endosomes and lysosomes.[44] Other workers have identified similar structures as compartments where antigenic peptide loading onto MHC class II binding sites occurs.[45,46] These vesicles, termed compartments for peptide loading (CPL) or Class II vesicles (CIIV), are considered components of the class II transport network and feature some characteristics of late endosomes and lysosomes, including acidic pH and proteolytic enzymes.[47]

Internalization of CD23 by IgE–antigen complexes

CD23 was cross-linked by IgE–NP complexes and, as a result, capping is evident even in samples kept at 4° (Fig. 7a). Optical sections of cells after 2 hr at 37° show fluorescent indentations originating from capped areas on the surface of B cells. These imply the beginning of IgE–antigen-induced endocytosis of the receptor (Fig. 7b). After 4 hr at 37°, strong accumulation of fluorescent label for CD23 in the cell cytoplasm is clearly evident (Fig. 7c). Strong cell surface fluorescence or capping are less common at this time point. The endocytosed label for CD23 appears strong and contained in areas of the cytoplasm close to the nucleus and is mostly detached from the remaining surface fluorescence.

After 6 hr at 37° (Fig. 7d), the progression from cytoplasmic to surface fluorescence is once more established and clearly evident. Furthermore, a large proportion of cells show strong cell surface fluorescence even after 6 hr incubation at 37°. The intensity of the fluorescent label for endocytosed CD23 and the association of cell surface and cytoplasmic fluorescence after 6 hr incubation at 37° suggest a recycling pathway induced by engaging of CD23 with IgE–antigen complexes. Incubation with antigen-free IgE at 37° appears to have no effect in inducing capping or endocytosis of CD23. Indeed, in cells incubated with IgE alone, fluorescent label for CD23 appears inert on the cell membrane after 2 hr at 37° (Fig. 7e). Lack of internalization was confirmed by flow cytometry following incubation with IgE for 0, 2·5 and 5 hr at 37° (results not shown). Cross-linking of the CD23–IgE cell surface complex by antigen is thus required for endocytosis.

Electrophoretic analysis of CD23 following endocytosis

Cell surface proteins on RPMI 8866 cells were iodinated, and duplicate sets of cells were incubated with or without CR3/43 for 18 hr at 37°. From each of the incubated cell populations, one sample of cells was acid-washed to remove non-covalently bound proteins from the surface and another was incubated with chymotrypsin to remove all surface proteins, for comparison with the untreated cell population. Cells were then lysed and CD23 was immunoprecipitated with anti-CD23 mAb BU38 conjugated to protein A agarose beads. Lysis and immunoprecipitation were followed by sodium dodecyl sulphate–polyacrylamide gel electrophoresis. This protocol allows the distinction between internal and external proteins, and external proteins that are either membrane-anchored or non-covalently bound to other surface proteins.
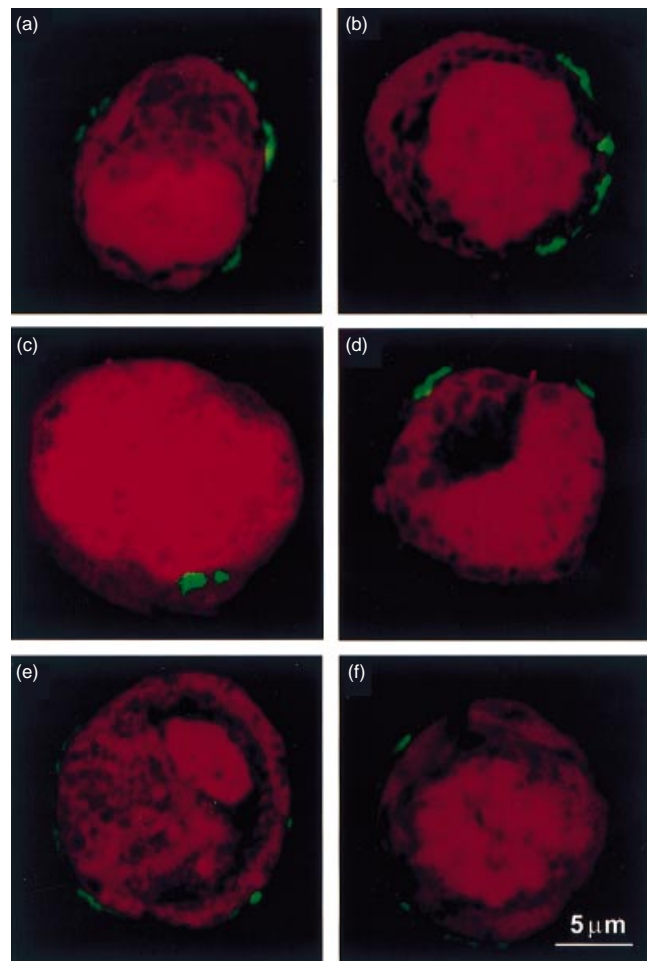
Figure 7. Endocytosis induced by an antigen–IgE complex in RPMI 8866 cells. Cells were incubated with EBVCS1 and anti-mouse IgG (Fab′)₂-FITC, followed by NP-IgE and NP-BSA. Propidium iodide was used to label nuclei and highlight the cell structure. Cells were kept on ice (a) or incubated at 37° for 2 hr (b), 4 hr (c), or 6 hr (d). Controls included a sample incubated with IgE without NP-BSA (e) and NP-BSA without IgE (f) that were incubated at 37° for 2 hr. Optical section thickness ∼ 1 μm.

Incubation of cells with the anti-HLA DR antibody CR3/43 at 37° for 18 hr caused partial conversion of CD23 to fragments of 37 000 and 33 000 MW (Fig. 8a,b, lane 2). These fragments were present on the cell surface since they were removed by chymotrypsin treatment (Fig. 8b, lane 4). These fragments of 37 000 and 33 000 MW were associated with the cell surface in a non-covalent manner, since they were removed by acid washing (Fig. 8a, lane 4). In the absence of CR3/43, these fragments were not formed (Fig. 8a,b, lanes 1 and 3).

In untreated cells, membrane (45 000) CD23 was processed into a fragment of 16 000 following incubation at 37° for 18 hr (Fig. 8a and Fig. 8b, lane 1). This fragment is constitutively accumulated inside the cell, and it has been reported that the rate of its formation is enhanced by antibodies to CD23.[48] The 16 000 fragment is removed neither by acid washing (Fig. 8a, lane 3) nor by chymotrypsin treatment (Fig. 8b, lane 3), indicating that it is not associated with the cell surface. Thus
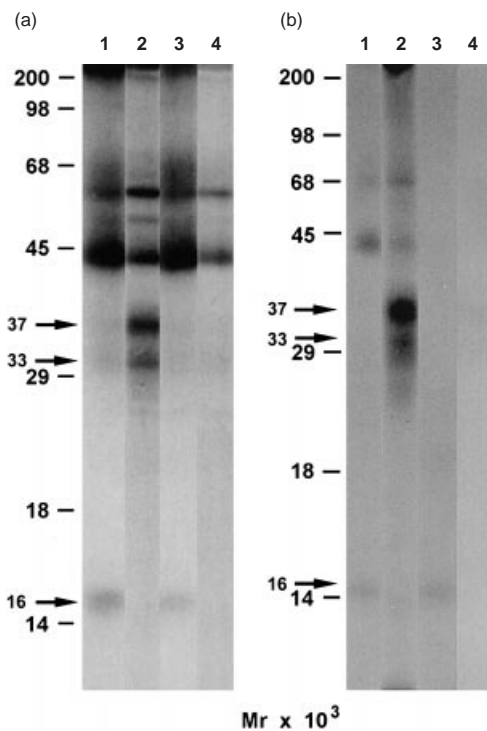
Figure 8. Electrophoretic analysis of intracellular and extracellular
[125]I-labelled CD23 from iodinated RPMI 8866 cells following
endocytosis induced by anti-HLA DR. Cells were incubated with or
without CR3/43 antibody for 18 hr at 37°. (a) Lane 1, CD23 from
untreated control cells; lane 2, cells treated with CR3/43; lane 3,
untreated control cells after acid washing; lane 4, cells treated with
CR3/43 and subjected to acid washing. (b) Lane 1, CD23 from
untreated control cells; lane 2, cells treated with CR3/43 antibody; lane
3, untreated control cells after chymotrypsin treatment; lane 4, cells
incubated with CR3/43 after chymotrypsin treatment.

incubation with CR3/43 inhibits the production of the intra-
cellular 16 000 CD23 fragment and promotes partial conver-
sion of the full length CD23 to fragments of 37 000 and 33 000
that are associated with the cell membrane in a non-covalent
manner.

DISCUSSION

We have shown here that CD23 may undergo two alternative
fates upon endocytosis in RPMI 8866 B cells. When cross-
linked by the anti-CD23 antibodies, BU38 or MHM6, it is
targeted into a degradative pathway. Our results are consistent
with those in previous work demonstrating that cross-linking
CD23 by BU38 leads to the transient formation of an inter-
mediate of 16 000 MW.[48,49] These fragments may be liberated
from the cell[50] or further degraded to peptides that can no
longer be detected by the anti-CD23 antibodies used in our
study. In contrast, cross-linking of HLA-DR by CR3/43, or
CD23 by an antigen–IgE complex, directs both HLA-DR and
CD23 into a recycling pathway, during which HLA-DR and
CD23 remain associated throughout. Upon cross-linking
by BU38, CD23 was observed in vesicles that resembled typical
late endosomes or lysosomes before disappearing from the
cells. In contrast, when CR3/43 was the cross-linker, CD23
could be seen in cytoplasmic organelles that resembled the

'compartments for peptide loading' (CPL) or 'class II vesicles'
(CIIV), described by previous authors.[45,47,51–54]

In the present work, the recycled CD23 at the cell surface
had also undergone partial cleavage to a fragment of 37 000. It
is likely that this fragment is equivalent to the 37 000 fragment
that is naturally released from CD23.[27] The fact that these
fragments could be removed by both chymotrypsin treatment
and acid washing of the cells indicates that they are non-
covalently bound to a component of the cell membrane. The
previously characterized 37 000 MW fragment retains a large
portion of the stalk and can form trimers.[4] It is therefore
possible that the fragments seen in this study represent
incompletely digested trimers, containing one or two chains
of full-length CD23, holding the 37 000 MW fragments in
place in the original trimers. The full-length chain(s) would
anchor the fragments on the cell surface under physiological
conditions. The pH 2·8 wash may then dissociate the trimers to
release the fragments. It is possible that the 37 000 MW frag-
ments may be an experimental artefact, since cross-linking here
was performed with an antibody against HLA-DR and CD23
was decorated with IOB8. It is known that IgE protects CD23
from cleavage.[55] Together these observations suggest that
CD23 would be recycled to the cell surface in the course of
facilitated antigen presentation.

During antigen presentation endocytosed antigen–antibody
complexes are targeted to CPL/CIIV. Newly synthesized MHC
Class II molecules enter CPL/CIIV from the Golgi, and are
thought to be the major source for antigen presentation.
However, MHC Class II molecules located at the cell surface
can also be transported to the endosomal network, participate
in peptide exchange and recycle to the cell surface.[56–63] The
time required for the recycling of HLA-DR with CD23 in the
present work, 3–6 hr, is consistent with the recycling time for
HLA-DR in B cells (∼ 4 hr) reported by previous authors.[60,64]
Simultaneous targeting of HLA-DR and antigen (bound to IgE
and in turn to CD23) to peptide loading compartments in the
endosomal network might be expected to facilitate peptide
loading of HLA-DR and thereby the process of antigen
presentation.

Once the CD23–HLA-DR complex returns to the cell
surface it may play another role in antigen presentation.
Previous studies have shown that antibodies to CD21 or CD23
inhibit antigen presentation,[21,22] consistent with co-localization
of the contacts between CD23 and CD21, and the T-cell
receptor/CD4 and MHC Class II/peptide, on the opposite cell
surfaces. Recent studies have indicated that antigen presenta-
tion is critically dependent on the duration of the B-cell–T-cell
interaction.[64,65] The stabilizing force of the CD23–CD21
interaction may therefore increase the probability of T-cell
activation. The CD23 stalk is 15 nm,[4] which is compatible with
its co-operation with HLA-DR in locking B cells to T cells.[65]

Both B cells and T cells express both CD23 and CD21, so
there is a question of the polarity of this interaction. Our results
suggest that CD23 on B cells may bind to CD21 on T cells.
T cells express lower levels of membrane-bound CD21 than
B cells,[66] but contain an equivalent concentration of mRNA
for CD21,[67] which could be rapidly translated into protein
and transported to the cell surface. In fact, CD21 appears to be
up-regulated in T cells during antigen presentation.[22]

The homology of CD23 to C-type lectins, which emerged
on sequencing the gene, was unexpected, since all other

known antibody Fc receptors are members of the immuno-globulin superfamily.[68] The C-type lectin family includes the asialoglycoprotein receptor (ASGPR), which functions in glycoprotein catabolism, mannose-binding protein, which functions in innate immunity, and selectins, which are involved in adhesion of inflammatory cells to the endothelium at sites of inflammation. The closest relative of CD23 in the C-type lectin family is ASGPR, and hence it is noteworthy that a molecule of ASGPR delivers an estimated 60 molecules of glycoprotein to lysosomes within the endosomal network of hepatoma cells.[69] The present results suggest that CD23 may promote the recycling of HLA-DR.

In summary, our results suggest that CD23 may be associated with HLA-DR in the process of recycling between the cell membrane and the endosomal network. Two features of this process may contribute to the efficiency of antigen presentation. Peptide exchange may be facilitated by the proximity of HLA-DR and antigen (bound to IgE and in turn to CD23) in peptide loading compartments of the endosomal network. The association of CD23 with HLA-DR at the surface of B cells may then help to stabilize specific B-cell–T-cell interactions, contributing to T-cell activation.

REFERENCES

1 Kikutani H, Suemura M, Owaki H *et al.* Fc epsilon receptor, a specific differentiation marker transiently expressed on mature B cells before isotype switching. J Exp Med 1986; **164:**1455–69.

2 Yokota A, Kikutani H, Tanaka T, Sato R, Barsumian EL, Suemura M, Kishimoto T. Two species of human Fcε receptor II (FcεRII/CD23): tissue-specific and IL-4 specific regulation of gene expression. Cell 1988; **55:**611–18.

3 Yokota A, Yukawa K, Yamamoto A, Sugiyama K, Suemura M, Tashiro Y, Kishimoto T, Kikutani H. Two forms of the low-affinity Fc receptor for the IgE differentially mediate endocytosis and phagocytosis: Identification of the critical cytoplasmic domains. Proc Natl Acad Sci USA 1992; **89:**5030–4.

4 Beavil AJ, Edmeades RL, Gould HJ, Sutton BJ. α-helical coiled-coil stalks in the low-affinity receptor for IgE (FcεRII/CD23) and related C-type lectins. Proc Natl Acad Sci USA 1992; **809:**753–7.

5 Beavil RL, Graber P, Aubonney N, Bonnefoy J-Y, Gould HJ. CD23/FcεRII and its soluble fragments can form oligomers on the cell surface and in solution. Immunology 1995; **84:**202–6.

6 Dierks SE, Bartlett WC, Edmeades RL, Gould HJ, Rao M, Conrad DH. The oligomeric nature of the murine FcεRII/CD23: implications for function. J Immunol 1993; **150:**2372–82.

7 Lawrence DA, Weigle WO, Spiegelberg HL. Immunoglobulins cytophilic for human lymphocytes, monocytes, and neutrophils. J Clin Invest 1975; **55:**368–87.

8 Aubry JP, Pochon S, Graber P, Jansen KU, Bonnefoy J-Y. CD21 is a ligand for CD23 and regulates IgE production. Nature 1992; **358:**505–7.

9 Lecoanet-Henchoz S, Gauchat J-F, Aubry JP *et al.* CD23 regulates monocyte activation through a novel interaction with the adhesion molecules CD11b-CD18 and CD11c-CD18. Immunity 1995; **3:**119–25.

10 Hermann P, Armant M, Brown E *et al.* The vitronectin receptor and its associated CD47 molecule mediates proinflammatory cyto-kine synthesis in human lymphocytes by interaction with soluble CD23. J Cell Biol 1999; **144:**767–75.

11 Kehry MR, Yamashita LC. Low affinity IgE receptor (CD23) function on mouse B cells: role in IgE-dependent antigen focusing. Proc Natl Acad Sci USA 1989; **86:**7556–60.

12 Pirron U, Schlunck T, Prinz JC, Rieber EP. IgE-dependent antigen focusing by human B lymphocytes is mediated by the low-affinity receptor for IgE. Eur J Immunol 1990; **20:**1547–51.

13 van der Heijden FL, Joost van Neerven RJ, van Katwijk M, Bos JD, Kapsenberg ML. Serum-IgE-facilitated allergen presentation in atopic disease. J Immunol 1993; **150:**3643–50.

14 Santamaria LF, Bheekha R, van Reijsen FC, Perez Soler MT, Suter M, Bruijnzeel-Koomen CA, Mudde GC. Antigen focusing by specific monomeric immunoglobulin E bound to CD23 on Epstein-Barr virus-transformed B cells. Hum Immunol 1993; **37:**23–30.

15 Squire CM, Studer EJ, Lees A, Finkelman FD, Conrad DH. Antigen presentation is enhanced by targeting antigen to the Fc epsilon RII by antigen-anti-FcεRII conjugates. J Immunol 1994; **152:**4388–96.

16 Gustavsson S, Hjulstrom S, Tianmin L, Heyman B. CD23/IgE-mediated regulation of the specific antibody response in vivo. J Immunol 1994; **152:**4793–800.

17 Fujiwara H, Kikutani H, Suematsu S *et al.* The absence of IgE antibody-mediated augmentation of immune responses in CD23-deficient mice. Proc Natl Acad Sci USA 1994; **91:**6835–9.

18 Mudde GC, Bheekha R, Bruijnzeel-Koomen CA. Consequences of IgE/CD23-mediated antigen presentation in allergy. Immunol Today 1995; **16:**380–3.

19 Westman S, Gustavsson S, Heyman B, Scand J. Early expansion of secondary B cells after primary immunization with antigen complexed with IgE. Immunology 1997; **46:**10–15.

20 Oshiba A, Hamelmann E, Haczku A, Takeda K, Conrad DH, Kikutani H, Gelfand EW. Modulation of antigen-induced B and T cell responses by antigen-specific IgE antibodies. J Immunol 1997; **159:**4056–63.

21 Flores-Romo L, Johnson GD, Ghaderi AA, Stanworth DR, Veronesi A, Gordon J. Functional implication for the topographical relationship between MHC class II and the low-affinity IgE receptor: occupancy of CD23 prevents B lymphocytes from stimulating allogeneic mixed lymphocyte responses. Eur J Immunol 1990; **20:**2465–9.

22 Grosjean I, Lachaux A, Bella C, Aubry JP, Bonnefoy J-Y, Kaiserlian D. CD23/CD21 interaction is required for presentation of soluble protein antigen by lymphoblastoid B cell lines to specific CD4+ T cell clones. Eur J Immunol 1994; **24:**2982–6.

23 Sarfati M, Delespesse G. Possible role of human lymphocyte receptor for IgE (CD23) or its soluble fragments in the in vitro synthesis of human IgE. J Immunol 1988; **141:**2195–9.

24 Sherr E, Macy E, Kimata H, Saxon A. Binding to the low affinity Fc epsilon receptor on B cells suppresses ongoing human IgE production. J Immunol 1989; **42:**481–9.

25 Saxon A, Kurbe-leamer M, Behle K, Max EE, Zhang K. Inhibition of human IgE production via FcεRII stimulation results from a decrease in the mRNA for secreted but not membrane H chains. J Immunol 1991; **147:**4000–6.

26 Yu P, Kosco-Vilbois M, Richards M, Kohler G, Lamers MC. Negative feedback regulation of IgE synthesis by murine CD23. Nature 1994; **369:**753–6.

27 Letellier M, Sarfati M, Delespesse G. Mechanisms of formation of human IgE binding factors (soluble CD23): I. FcεRII bearing B cells generate IgE binding factors of different molecular weights. Mol Immunol 1989; **26:**1105–12.

28 Marolewski AE, Buckle DR, Christie G, Earnshaw DL, Flamberg PL, Marshall LA, Smith DG, Mayer RJ. CD23 (FcεRII) release from cell membranes is mediated by a membrane-bound metallo-protease. Biochem J 1998; **333:**573–9.

29 Gordon J, Cairns JA, Milsum MJ, Gillis S, Guy G. Interleukin-4 and soluble CD23 as progression factors for human B-lymphocytes: analysis of their interactions with agonists of the phosphoinositide 'dual pathway' of signalling. Eur J Immunol 1988; **18:**1561–5.

30 Liu Y-J, Carins JA, Holder MJ, Abbot SD, Jansen KU, Bonnefoy J-Y, Gordon J, MacLennan IC. Recombinant 25 kD CD23 and interleukin 1α promote the survival of germinal centre B cells: evidence for the bifurcation of development of centrocytes rescued from apoptosis. Eur J Immunol 1991; **21:**1107–14.

31 Mossalayi MD, Lecron JC, Dalloul AH, Sarfati M, Bertho JM, Hofstetter H, Delespesse G, Debre P. Soluble CD23 (FcεRII) and interleukin-1 synergistically induce early human thymocyte maturation. J Exp Med 1990; **171:**959–64.

32 Bertho JM, Fourcade C, Dalloul AH, Debré P, Mossalayi MD. Synergistic effect of interleukin 1 and soluble CD23 on the growth of human CD4+ bone marrow-derived T cells. Eur J Immunol 1991; **21:**1073–6.

33 Mossalayi MD, Arock M, Bertho JM, Blanc C, Dalloul AH, Hofstetter H, Sarfati M, Delespesse G. Proliferation of early human myeloid precursors induced by interleukin-1 and recombinant CD23. Blood 1990; **75:**1924–7.

34 Reljic R, Cosentino G, Gould HJ. Function of CD23 in the response of human B cells to antigen. Eur J Immunol 1997; **27:**572–5.

35 Gould HJ, Beavil RL, Reljic R, Shi J, Ma CW, Sutton BJ, Ghirlando R. IgE homeostasis: is CD23 the safety switch? In: Vercelli D, eds. IgE Regulation: Molecular Mechanisms Chichester: John Wiley Ltd, 1997:38–59.

36 Bonnefoy J-Y, Guillot O, Spits H, Blanchard D, Ishizaka K, Banchereau J. The low affinity receptor for IgE (CD23) on B lymphocytes is spatially associated with HLA DR antigens. J Exp Med 1988; **167:**57–72.

37 Kijimoto-Ochiai S, Noguchi A. Two peptides from CD23, including the inverse RGD sequence and its related peptide, interact with the MHC class II molecule. Biochem Biophys Res Commun 2000; **267:**686–91.

38 Neuberger MS, Williams GT, Mitchell EB, Jouhal SS, Flanagan JG, Rabbitts TH. A hapten-specific chimaeric IgE antibody with human physiological effector function. Nature 1985; **314:**268–70.

39 Brodsky FM, Koppelman B, Blum JS, Marks MS, Cresswell P, Guagliardi L. Intracellular co-localization of molecules involved in antigen processing and presentation by B cells. Cold Spring Harbor Symposium. Quant Biol 1989; **LIV:**319–31.

40 Lew AM, Margulies DH, Maloy WL, Lillehoj EP, McCluskey J, Coligan JE. Alternative protein products with different carboxyl termini from a single class I gene, H-2 kb. Proc Natl Acad Sci USA 1986; **83:**6084–8.

41 Schwartz-Albiez B, Moldenhauer G. Immunochemistry and epitope analysis using CD10, CD19, CD20, CD21, CD23, CD24, CD37, CD38, CD39, and CD40 mAb. In: Knapp W, Dorken B, Gilks WR, et al. eds. Leukocyte Typing IV White Cell Differentiation Antigens. Oxford: Oxford University Press, 1989:142–54.

42 Gordon J, Webb AJ, Guy GR, Walker L. Triggering of B lymphocytes through CD23: epitope mapping and studies using antibody derivatives indicate an allosteric mechanism of signalling. Immunology 1987; **60:**517–21.

43 Bonnefoy J-Y, Aubry JP, Peronne C, Wijdenes J, Banchereau J. Production and characterization of a monoclonal antibody specific for the human lymphocyte low affinity receptor for IgE: CD23 is a low affinity receptor for IgE. J Immunol 1987; **138:**2970–8.

44 Pulczinski S, Bosen AM, Jensen OM. Modulation and intracellular transport of CD20 and CD21 antigens induced by B1 and B2 mono-clonal antibodies in Raji and Jok-1 cells – an immunofluorescence and immunoelectron microscopy report. Leukemia Res 1994; **18:**541–52.

45 Amigorena S, Drake R, Webster P, Mellman I. Transient accumu-lation of new class II MHC molecules in a novel endocytic compartment in B lymphocytes. Nature 1994; **369:**113–20.

46 Sanderson F, Kleijmeer MJ, Kelly A, Verwoerd D, Tulp A, Neefjes JJ, Geuze HJ, Trowsdale J. Accumulation of HLA DM, a regulator of antigen presentation in MHC class II compartments. Science 1994; **266:**1566–9.

47 Gueze HJ. The role of endosomes and lysosomes in MHC class II functioning. Immunol Today 1998; **10:**282–7.

48 Grenier-Brossette N, Bourget I, Akoundi C, Bonnefoy J-Y, Cousin JL. Spontaneous and ligand-induced endocytosis of CD23 (Fcε receptor II) from the surface of B lymphocytes generates a 16-kDa intracellular fragment. Eur J Immunol 1992; **22:**1573–7.

49 Munoz O, Brignone C, Grenier-Brossette N, Bonnefoy J-Y, Cousin JL. Binding of anti-CD23 monoclonal antibody to the leucine zipper motif of FcεRII/CD23 on the B cell membrane promotes its proteolytic cleavage. J Biol Chem 1998; **273:**31795–80.

50 Lee BW, Simmons CF, Wileman T, Geha RA. Intracellular cleavage of newly synthesized low affinity FcεRII provides a second pathway for the generation of the 28 kDa soluble FcεRII fragment. J Immunol 1989; **142:**1614–20.

51 Drake JR, Webster P, Cambier JC, Mellman I. Delivery of B cell receptor-internalized antigen to endosomes and class II vesicles. J Exp Med 1997; **186:**1299–306.

52 Pierre P, Mellman I. Exploring the mechanisms of antigen processing by cell fractionation. Curr Opinion Immunol 1998; **10:**145–53.

53 Tulp A, Verwoerd D, Dobberstein B, Ploegh HL, Pieters J. Isolation and characterization of the intracellular MHC class II compartment. Nature 1994; **369:**120–6.

54 West MA, Lucocq JM, Watts C. Antigen processing and class II MHC peptide loading compartments in human B lymphoblastoid cells. Nature 1994; **369:**147–51.

55 Lee WT, Rao M, Conrad DH. The murine lymphocyte receptor for IgE. IV.The mechanism of ligand-specific receptor upregulation on B cells. J Immunol 1987; **139:**1191–8.

56 Harding CV, Roof RW, Unanue ER. Turnover of Ia-peptide complexes is facilitated in viable antigen-presenting cells: biosyn-thetic turnover of Ia vs peptide exchange. Proc Natl Acad Sci USA 1989; **86:**4230–4.

57 Harding CV, Unanue ER. Antigen processing and intracellular Ia. Possible roles of endocytosis and protein synthesis in Ia function. J Immunol 1989; **142:**12–9.

58 Adorini L, Appella E, Doria G, Cardiaux F, Nagy ZA. Competition for antigen presentation in living cells involves exchange of peptides bound by class II MHC molecules. Nature 1989; **342:**800–3.

59 Reid PA, Watts C. Constitutive endocytosis and recycling of major histocompatibility complex class II glycoproteins in human B-lymphoblastoid cells. Immunology 1992; **77:**539–42.

60 Pinet V, Malnati MS, Long EO. Two processing pathways for the MHC class II-restricted presentation of exogenous influenza virus antigen. J Immunol 1994; **152:**4852–60.

61 Pinet V, Vergelli M, Martin R, Bakke O, Long EO. Antigen presentation mediated by recycling of surface HLA-DR molecules. Nature 1995; **375:**603–6.

62 Escola JM, Deleuil F, Stang E, Boretto J, Chavrier P, Gorvel JP. Characterization of a lysozyme-major histocompatibility complex class II molecule-loading compartment as a specialized recycling endosome in murine B lymphocytes. J Biol Chem 1996; **271:**27360–5.

63 Griffin JP, Chu R, Harding CV. Early endosomes and a late endocytic compartment generate different peptide-class II MHC complexes via distinct processing mechanisms. J Immunol 1997; **158:**1523–32.

64 Valitutti S, Dessing M, Aktories K, Gallati H, Lanzavecchia A. Sustained signalling leading to T cell activation results from prolonged T cell receptor occupancy. Role of T cell actin cytoskeleton. J Exp Med 1995; **181:**577–84.

65 Shaw AS, Dustin ML. Making the T cell receptor go the distance: a topological view of T cell activation. Immunity 1997; **6:**361–9.

66 Fischer E, Belibrias C, Kazatchkine MD. Expression of CR2 (the C3dg/EBV receptor, CD21) on normal human peripheral blood T lymphocytes. J Immunol 1991; **146:**865–9.

67 Braun M, Melchers I, Peter HH, Illges H. Human B and T lymphocytes have similar amounts of CD21 mRNA, but differ in surface expression of the CD21 glycoprotein. Int Immunol 1998; **10:**1197–202.

68 Sutton BJ, Gould HJ. The human IgE network. Nature 1993; **366:**421–8.

69 Schwartz AL, Fridovich SE, Lodish HF. Kinetics of internalization and recycling of the asialoglycoprotein receptor in a hepatoma cell line. J Biol Chem 1982; **257:**4230–7.